Biochemistry

Article

Cite This: Biochemistry 2017, 56, 6575−6584

pubs.acs.org/biochemistry

Quantitative Study of the Oligomerization of Yeast Prion Sup35NM Proteins

Yanjing Wang*,† and Chi Wu†,‡

†Department of Chemistry, The Chinese University of Hong Kong, Shatin, N.T., Hong Kong, China

‡Hefei National Laboratory for Physical Sciences at the Microscale, Department of Chemical Physics, University of Science and Technology of China, Hefei, Anhui 230026, China

ABSTRACT: The fibrillation of misfolded neurodegenerative disease-related proteins has been extensively studied over the past few decades, but the initial oligomerization has been rarely examined even though some recent evidence indicated that small protein oligomers are more neurotoxic than long protein fibers. It is rather difficult to study the initial oligomerization (nucleation) because most experimental methods, such as the β-sheet-related fluorescence assay and X-ray diffraction, are unable to detect small structureless protein oligomers. In this study, we have successfully developed a method to link a short thermally sensitive poly(*N*-isopropylacrylamide) (PNIPAM) chain to a model protein, Sup35NM, at a specific 31st residue site (Sup35NM-31m-PNIPAM) via the efficient thiol−ene Michael addition reaction. The oligomerization was studied by a combination of laser light scattering, the thioflavin T assay, and transmission electron microscopy. We found that the lag phase of Sup35NM was delayed from 12 to >24 h under the physiological condition after the PNIPAM linkage. The oligomerization and fibrillation constants decreased from 5.0×10^{-3} to 1.5×10^{-3} h^{-1} and from 3.0×10^{-2} to 1.8×10^{-2} μM^{-1} h^{-1}, respectively, presumably because of the steric hindrance introduced by the PNIPAM chain. Moreover, after initiating the oligomerization, we found that the oligomer distribution in the first 6 h repeatedly and quantitatively follows the Smoluchowski coagulation model. Our study paves the way for controllably and quantitatively studying the oligomerization kinetics of amyloidogenic proteins. In addition, by investigating the effects of different small molecules on the oligomerization kinetics, we should be able to screen potential drugs to slow the development of neurodegenerative diseases.

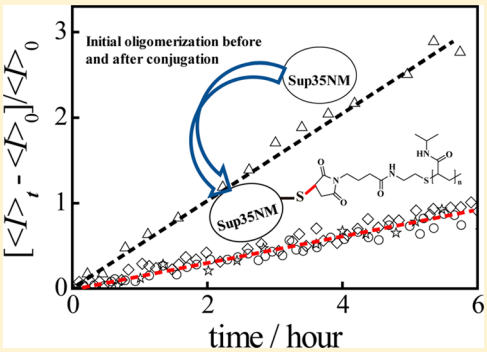

A protein chain can fold into a specific three-dimensional structure to acquire its biological functions. The folding process includes a series of complicated steps that can be affected by various internal and external factors, including its amino acid sequence and environment.[1,2] The misfolded protein chains could become the origins of a wide range of diseases. There is sufficient evidence to correlate protein misfolding and aggregation with many neurological diseases,[3] including Alzheimer's disease (AD), Parkinson's disease (PD), Huntington's disease (HD), and type II diabetes. A common pathological hallmark of these diseases is the formation of a fibrillar protein aggregate named amyloid. Amyloid fibrils are physically stable with a characteristic cross-β structure.[4−6] Patients with neurodegenerative diseases usually lose their abstract thinking, skilled movement, cognition, and other self-care ability. AD alone affects more than 35 million people worldwide, accompanied by a dramatic increase as the population ages.[7,8] Because of the lack of clinically efficient drugs that can halt or even slow the propagation of the disease, it has been considered an incurable disease.[9,10] Therefore, it is of great significance to find a way to develop a reliable quantitative method for screening potential drugs for the treatment of neurodegenerative diseases.

Over the past two decades, a tremendous amount of effort has been devoted to the search for active compounds that can inhibit fibril formation or disrupt prion propagation in the infected mouse to extend its life span.[11−13] At the same time, different chemicals or chaperones as inhibitors have shown some potential abilities to slow amyloid propagation both *in vitro* and *in vivo*.[14−19] However, their interaction mechanism at the molecular level is unclear.[20] Physically, the fibril formation of misfolded proteins is a process with two distinct steps,[7] nucleation and crystallization, in other words, the oligomerization of a limited number of misfolded proteins, resulting in small structureless interchain aggregates, and the formation of fibrils with an ordered structure that can be detected via X-ray diffraction. Small oligomers formed in the initial stage are metastable;[21] association and dissociation occur constantly, leading to small aggregates (nuclei) with different sizes and morphologies.[22] When the size of one oligomer reaches a critical value, the crystallization (fibril formation) process starts.[3,5,6,23] More recent evidence suggested that small oligomers were more neurotoxic and could be the primary culprit that causes neuronal dysfunction and cell death.[24]

Received: September 27, 2017
Revised: November 16, 2017
Published: November 23, 2017

DOI: 10.1021/acs.biochem.7b00966
Biochemistry 2017, 56, 6575−6584

In the nucleation process, it could take days, months, or even years (e.g., in the development of a neurodegenerative disease) for small oligomers to reach the critical size, depending on how high the interaction energy (ΔE) is.[25,26] More precisely, the induction period or the lag time (Δt) is related to ΔE as $\Delta t \sim 1/\{\exp[\Delta E/(k_B T)] - 1\}$, where k_B is the Boltzmann constant. In principle, a very small decrease in ΔE could significantly prolong the induction period, which provides us a potentially rational therapeutic strategy. Namely, instead of stopping or reversing the fibril formation process, we can search for small molecular drugs that can effectively interact with the protein chains to decrease the interaction energy among the protein chains and prolong the lag time, as suggested by Jarrett and Lansbury.[27] Because most neurodegenerative diseases occur late in life,[28] delaying the onset of the disease would greatly improve the potential patient's quality of life and even make the clinical treatments unnecessary. Note that this is a promising approach that has rarely been touched experimentally, in which the oligomerization process is distinguished and studied in detail.

However, how to find such small molecular drugs is problematic. First, we were not able to conduct a long-term clinic trial over a period of ≥30 years to determine whether a small molecular drug has an effect on prolonging the lag time. Therefore, establishing a repeatable and quantitative method for screening out small molecular drugs that can prolong the lag time is critically important in such an approach. However, the previously reported high-throughput *in vitro* drug screening assay focuses on only the formation of large aggregates, and there might be false positive results if the chemicals are not able to delay the nucleation process but can delay the propagation process.[29] Second, the transient oligomers are heterogeneous and structureless,[8,21] so that it is rather difficult, if not impossible, to study the oligomerization process via cross-β structure-based traditional methods, such as the thioflavin T (ThT) dye fluorescence assay, the Congo red spectral shift assay, and X-ray diffraction.[30−32] To the best of our knowledge, only laser light scattering (LLS) can quantitatively detect the formation of small oligomers formed during the nucleation process (lag phase) because the scattered light intensity is proportional to the square of the mass of a scattering object, which is very sensitive even to the formation of a trace amount of small oligomers. This is why we decide to combine it with other existing methods to follow the oligomerization, i.e., protein−protein association in the very initial stage, prior to the formation of fibrils.

To prevent infection with pathogenic prions, we chose a model protein, Sup35, a domain of the translation termination protein in *Saccharomyces cerevisiae*, similar to human prion, to conduct the proof-of-concept research. Sup35 can transfer from an active soluble state to an inactive amyloidogenic state with a fibrillar structure,[33,34] safe to humans and infectious to only yeasts, which is widely accepted in the study of amyloid formation and characterization of the fibril structure.[35−37] Sup35 contains three different regions, namely, N, M, and C, based on different functions and positions. The asparagine- and glutamine-rich N region (residues 1−123) determines the aggregation behavior. The next highly charged M region (residues 124−253) enhances the protein solubility. The C region (residues 254−685) has a translation termination function in yeast.[36,37] It has been recognized that the N and M domains encode the prion-like function because the purified Sup35NM without the C region can form the amyloid structure in physiologic buffer, making it suitable for laboratory study.[23,38] Previously, Lindquist and co-workers created a series of cysteine-substituted mutations throughout Sup35NM and showed that such mutated Sup35NM chains can still form amyloid structure. Using a pyrene-modified mutated Sup35NM, they proposed a well-accepted β-helix model for the prion amyloid structure.[23,39] Moreover, they found that there are intermolecular interactions between the 31st residues on protein Sup35NM, which provided us a promising candidate site for protein engineering.

Note that wild-type Sup35NM proteins aggregate immediately upon being diluted under physiological conditions at or below room temperature (~25 °C), so that there is not sufficient time to perform a detailed study of the initial oligomerization. To overcome such a problem, we decided to conjugate a thermally sensitive short water-soluble poly(*N*-isopropylacrylamide) (PNIPAM) chain with a maleimide end group to a specific protein site to increase its solubility and modulate its activity.[40,41] PNIPAM is soluble in water only below ~32 °C,[42,43] so that we can prepare the protein solution at lower temperatures to increase the protein solubility and study the oligomerization at certain temperatures over a specific period. The conjugation was performed with a high efficiency (~87%) via the thiol−ene click chemistry between the thiol group on a cysteine residue and the carbon−carbon double bond on maleimide with tris(2-carboxyethyl)phosphine (TCEP) as a reductant to remove the possible disulfide bond formed between two protein molecules and an an activator for the subsequent thiol−ene reaction[44,45] under mild conditions.[46] The conjugation of a polymer chain to a protein chain can alter the solubility, stability, and biocompatibility of the protein, which has been widely employed for applications in medicine and biotechnology.[47,48]

Also difficult is making a true protein solution in which all protein chains are molecularly dispersed. Previously, after trying all the existing solution preparation protocols, we always found a trace amount of small undissolved oligomers in the solutions as determined by dynamic LLS measurements even in the presence of high concentrations of different denaturants. Physically, those small oligomers may serve as the nucleation agents, i.e., the crystallization seeds, in the initial stage of fibril formation.[49] The existence of different trace amounts of small oligomers leads to different kinetic processes even for the protein solutions with an identical initial concentration,[36,50,51] making the study of the initial oligomerization impossible. Our previous study found that ultrafiltration using a 20 nm membrane filter could completely remove those small undissolved oligomers so that each time we could start from a true solution of Sup35NM.[52]

MATERIALS AND METHODS

Materials. The LB broth, kanamycin sulfate, isopropyl β-D-1-thiogalactopyranoside (IPTG), guanidine hydrochloride (GdmCl), Tris-HCl, imidazole, sodium phosphate, sodium hydrogen phosphate, ammonium persulfate (APS), tetramethylethylenediamine (TEMED), and sodium dodecyl sulfate (SDS) were purchased from USB and used without further purification. TCEP, 5,5-dithiobis(2-nitrobenzoic acid) (DTNB), ThT dye, maleimide-terminated PNIPAM, and uranyl acetate were purchased from Sigma-Aldrich. A 30% acrylamide/bisacrylamide solution and Coomassie Brilliant Blue R-250 dye were purchased from Bio-Rad. Prestained Protein Ladder and the bicinchoninic acid (BCA) protein assay

DOI: 10.1021/acs.biochem.7b00966
Biochemistry 2017, 56, 6575−6584

kit were products of Thermo Scientific. The HisTrap HP column and beads were from GE Healthcare (Uppsala, Sweden). The membrane filters with different pore sizes were purchased from Whatman. The ultrafiltration device for concentrating samples was obtained from Millipore.

Protein Expression and Purification. Expression of Sup35NM or Sup35NM-31m (mutated at residue 31 in the N region) was performed using *Escherichia coli* BL21 (DE3). Each corresponding gene with a His tag at the end of the M region (six histidines) was cloned in the pET28a vector. The bacteria were cultured in LB medium supplemented with 50 μg/mL kanamycin. Protein expression was induced after the addition of 1 mM IPTG once the optical intensity of the bacterial solution measured at a wavelength of 600 nm (OD_{600}) had reached a value of 0.5. The bacteria were further allowed to grow at 37 °C for 4 h. To purify the target protein, we lysed the harvested bacteria with binding buffer [8 M GdmCl buffer, 40 mM imidazole, and 20 mM Tris (pH 7.4)] overnight at room temperature. The lysate was then centrifuged at 20000*g* for 1.5 h. The supernatant was filtered with a 220 nm membrane and then applied to the HisTrap HP column or beads for purification by following the manufacturer's protocol. After purification, the wild-type Sup35NM protein was eluted from the column with elution buffer [8 M GdmCl buffer, 500 mM imidazole, and 20 mM Tris (pH 7.4)], passing through a 20 nm membrane filter to obtain a true monomeric protein solution.[52] The protein solution was further concentrated using a centrifugal filter unit with nominal molecular weight limits (NMWLs) of 10 and 3 kDa before being subjected to dilution to initiate protein association. For the mutated variant Sup35NM-31m, HisTrap HP beads were used for purification. The protein bound to beads was directly used for further reaction before elution and preparation of the sample solution.

Conjugation of PNIPAM to Protein Sup35NM-31m. PNIPAM terminated with a maleimide group was dissolved in 4 M GdmCl buffer with 5 mM TCEP. The pH value of the solution was adjusted to 8.0 with 1 M NaOH after dissolution. The PNIPAM solution was then mixed with the nickel beads to which Sup35NM-31m protein had bound. The molar ratio of PNIPAM to protein Sup35NM-31m was 300:1. The reaction was conducted at 12 °C with slow stirring to prevent possible protein degradation. Samples at different reaction time intervals were taken to check the reaction conversion. After 48 h, the supernatant PNIPAM solution was removed from the reaction system to stop the reaction. The nickel beads were then washed with 10 volumes of 4 M GdmCl buffer to thoroughly remove the unreacted PNIPAM and TCEP. Subsequently, the beads were immersed in 8 M GdmCl buffer followed by elution with 8 M GdmCl elution buffer to obtain the Sup35NM-31m−PNIPAM conjugate. The monomeric conjugate solution was prepared and concentrated by using the same method that was used for wild-type Sup35NM.

Characterization of the Sup35NM-31m−PNIPAM Conjugate. First, the reaction product was checked by sodium dodecyl sulfate−polyacrylamide gel electrophoresis (SDS−PAGE). The SDS−PAGE sample loading dye containing 2% (w/v) SDS was added to nickel beads with protein Sup35NM-31m or the conjugate bound. The samples were analyzed after incubation at 85 °C for 5 min by 15% SDS−PAGE. Then, the samples were analyzed by matrix-assisted laser desorption ionization time-of-flight mass spectrometry (MALDI-TOF MS). For sample preparation, the target protein was eluted from the nickel beads, precipitated with isopropanol, and then dissolved in a 70% acetonitrile/0.3% trifluoroacetic acid mixture by vortexing. Afterward, an equal volume of α-cyano-4-hydroxycinnamic acid (CHCA) was added as the matrix. Finally, the mixture was spotted onto the target plate and analyzed in reflector mode, using a mass spectrometer (Bruker Autoflex Speed).[53]

BCA Protein Assay and Modified Ellman Assay. A combination of the BCA protein assay and the modified Ellman assay were further used to quantify the conjugation efficiency. First, the protein concentration was determined by the BCA protein assay (Pierce BCA Protein Assay Kit, ThermoScientific) following the manufacturer's procedure. Once we knew the concentrations of Sup35NM-31m and the Sup35NM-31m−PNIPAM conjugate, we determined the total free sulfhydryl group in the same amount of a Sup35NM-31m bead suspension before and after conjugation with PNIPAM using a modified Ellman assay to calculate the conjugation efficiency. Briefly, $NaBH_4$ [30% (w/w) in 1 M NaOH] was used as the reducing agent to cleave all the possible disulfide bonds in the samples by incubating the protein solution in 8 M GdmCl buffer for 30 min at 42 °C. An antifoam agent, hexanol, was added after the reducing reaction to remove the foams produced. A 6 M HCl solution was further added dropwise to remove the excess sodium borohydride, and the pH of the solution was adjusted to 8.0. Finally, Ellman's reagent, DTNB dissolved in methanol, was added to the suspension. The reaction mixture was shaken for 15 min at room temperature. The absorbance of the reaction solution was measured at 415 nm using a microplate reader (Bio-Rad), and the conjugation efficiency was calculated as $(SH_{total} - SH_{free})/SH_{total} \times 100\%$, where SH_{total} and SH_{free} were determined before and after the conjugation reaction, respectively.

ThT Fluorescence Assay. The well-established ThT fluorescence assay was used to identify and quantify the formation of amyloid fibrils *in vitro* as described previously.[31,54] The concentrated monomeric solution of Sup35NM or the Sup35NM-31m−PNIPAM conjugate in 8 M GdmCl buffer was quickly diluted 200-fold into phosphate-buffered saline (PBS) (0.1 M, pH 7.4) to initiate protein association. The ThT stock solution was added immediately after protein dilution to a final concentration of 10 μM. The fluorescence intensity of the solution was then measured in triplicate at different time intervals by a fluorescence spectrophotometer (HITACHI F-7000) using a slit width of 5 nm for excitation and emission. A wavelength of 450 nm was used to excite the ThT dye, and the fluorescence emission was recorded from 460 to 520 nm with a maximum peak at 490 nm.[51] Before each measurement, the solution was slightly stirred to keep the solution homogeneous.

Transmission Electron Microscopy (TEM). The freeze-drying method was adopted for sample preparation for TEM imaging.[55] A 10 μL portion of the protein solution taken at different times after dilution was placed on the cupper grid and frozen quickly by immersion in liquid nitrogen. The frozen sample on the cupper grid was then freeze-dried for ~3 h. The dried sample was then subsequently stained with 10 μL of 1% uranyl acetate for 1 min and blotted gently with filter paper. The sample was further washed with deionized water twice and dried in the air. TEM imaging was performed on an FEI CM120 microscope operated at 120 kV.

Laser Light Scattering (LLS). A commercial LLS spectrometer (ALV/DLS/SLS-5022F) equipped with a multi-τ digital time correlator (ALV5000) and a vertically polarized 22 mW He−Ne cylindrical laser (λ_0 = 632.8 nm; Uniphase)

DOI: 10.1021/acs.biochem.7b00966
Biochemistry 2017, 56, 6575−6584

was used. The detailed LLS theory can be found elsewhere.[56−58] In static LLS, the excess absolute time-averaged scattered light intensity at a given scattering vector q, known as the excess Rayleigh ratio, $R_{vv}(q)$, of a dilute polymer solution at a concentration C (grams per milliliter) is related to the weight-average molar mass (M_w), the root-mean-square z-average radius of gyration ($\langle R_g^2\rangle_z^{1/2}$) (or written as $\langle R_g\rangle$), and the second virial coefficient (A_2) as

$$\frac{KC}{R_{vv}(q)} \approx \frac{1}{M_w}\left(1 + \frac{1}{3}\langle R_g^2\rangle_z q^2\right) + 2A_2C \quad (1)$$

where $K = 4\pi^2 n^2 (dn/dC)^2/(N_A\lambda_0^4)$ and $q = 4\pi n \sin(\theta/2)/\lambda_0$ with N_A, dn/dC, n, θ, and λ_0 being Avogadro's number, the specific refractive index increment, the solvent refractive index, the scattering angle, and the wavelength of the incident light in vacuum, respectively. When both C and q are sufficiently small, eq 1 can be simplified as

$$\frac{R_{vv}(q)}{KC} \approx M_w \quad (2)$$

where $C = W/V$ and M_w is defined as $(\sum W_i M_i)/W$; therefore, $\langle I_s(q \to 0)\rangle \propto \sum W_i M_i = \sum n_i M_i^2$, where W_i, n_i, and M_i are the mass, number, and molar mass of the ith scattering object, respectively. Thus, $\langle I_s(q \to 0)\rangle \propto M^2$. Namely, the scattering intensity is very sensitive to protein association.

In dynamic LLS, the measured normalized intensity−intensity time correlation function, $G^{(2)}(q,t) \equiv \langle I(q,0)I(q,t)\rangle$, where $I(q,t)$ is the scattering intensity at a given scattering vector (q) and a given delay time (t), is related to normalized electric field−field time correlation function $g^{(1)}(q,t)$ by the Siegert relation as

$$G^{(2)}(q,t) = A[1 + \beta|g^{(1)}(q,t)|^2] \quad (3)$$

where A $[=\langle I(q,0)\rangle^2]$ is the measured baseline and β is the coherent factor, depending on the detection optics. For a polydisperse system, $|g^{(1)}(q,t)|$ is generally related to a characteristic line width distribution $G(\Gamma,q)$ as follows

$$|g^{(1)}(q,t)| = \int G(\Gamma,q)e^{-\Gamma(q)t}\,d\Gamma \quad (4)$$

$G(\Gamma,q)$ can be calculated from the Laplace inversion of each measured $G^{(2)}(q,t)$ using the CONTIN program provided by ALV. For a purely diffusive process, the plot of Γ versus q^2 is a straight line passing through the origin and the slope is the average translational diffusion coefficient constant ($\langle D\rangle$) of the scattering objects. The hydrodynamic radius ($\langle R_h\rangle$) can be calculated by using the Stokes−Einstein equation, $R_h = k_BT/(6\pi\eta D)$, where k_B, T, and η are the Boltzmann constant, the absolute temperature, and the viscosity, respectively. All the LLS experiments were performed at 25 °C.

RESULTS AND DISCUSSION

Preparation of the Sup35NM-31m−PNIPAM Conjugate. To prepare the well-defined protein−polymer conjugate, cysteine introduction is widely employed.[47,59] In general, this method can be applied to proteins with very few, if any, cysteines that do not participate in disulfide bond formation.[60] In the study presented here, a targeted cysteine was introduced at position 31 of Sup35NM by site-directed mutagenesis to obtain a mutant Sup35NM-31m that can be conjugated with a short commercially available PNIPAM chain with a functional maleimide end via thiol−ene click chemistry.[61] The conjugation, as shown in Scheme 1, increases the solubility of Sup35NM at lower temperatures and enables us to induce the association of Sup35NM with a well-defined starting point.

Scheme 1. Synthetic Scheme for Conjugating the Sup35NM-31m Protein with a Maleimide-Terminated PNIPAM Chain on a Nickel Bead[a]

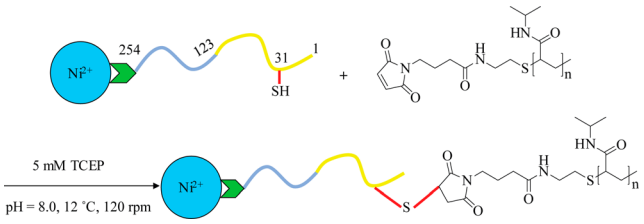

[a]The reaction was performed at 12 °C with a shaking speed of 120 rpm.

To improve the efficiency of conjugation between the maleimide and thiol groups, we used TCEP as a reducing agent and as an activator[60] in the presence of an excess of PNIPAM chains. To facilitate the purification of the resultant conjugated Sup35NM-31m, we attached Sup35NM-31m on small nickel beads because those unreacted free PNIPAM molecules can be efficiently washed out with the reaction buffer. Note that the existence of remaining free PNIPAM chains would influence our study of protein oligomerization and association. The conjugation efficiency was checked by a 15% SDS−PAGE gel that had been stained with Coomassie Brilliant Blue R-250.

Figure 1 shows the retardation and smearing of the bands at different reaction times, leading to the estimation of a

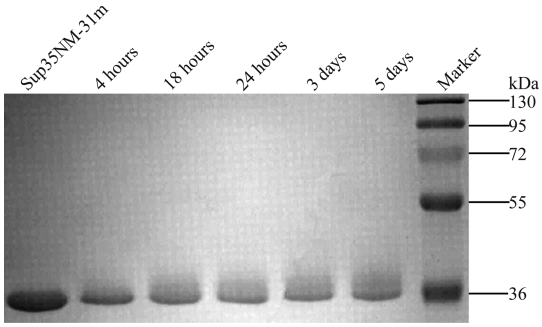

Figure 1. Typical SDS−PAGE (15%) result for both purified Sup35NM-31m protein and its PNIPAM conjugate after different indicated reaction times. The right lane contained the molar mass standards.

conjugation efficiency of ∼87% determined by a combination of the BCA protein assay and the modified Ellman assay. The successful conjugation was further confirmed by MALDI-TOF MS, as shown in Figure 2, based on a significant right shift of the MALDI-TOF peak to a higher molar mass with m/z ∼822 Da after the conjugation. Moreover, the peak changes from a single peak (Sup35NM-31m) to multiple peaks (Sup35NM-31m−PNIPAM conjugates) because the PNIPAM used does not have a uniform chain length distribution.

Preparation of a True Protein Solution. In a true solution, protein chains are molecularly dispersed inside a solvent without any interchain association, which is the starting point of our study of the initial stage of the protein association (oligomerization). Previously, a high concentration of urea or

DOI: 10.1021/acs.biochem.7b00966
Biochemistry 2017, 56, 6575−6584

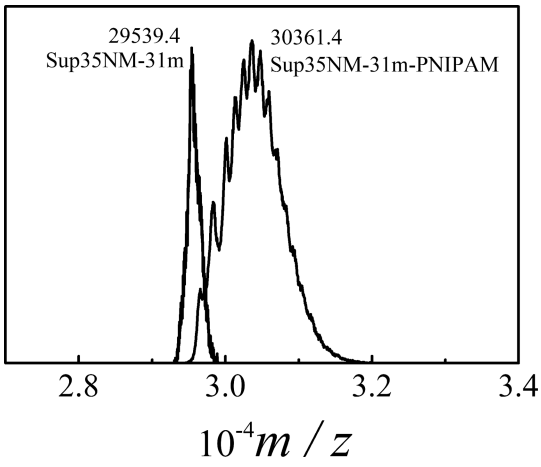

Figure 2. MALDI-TOF MS spectroscopy of Sup35NM-31m and the Sup35NM-31m−PNIPAM conjugate, where a 70% acetonitrile/0.3% trifluoroacetic acid mixture and CHCA were used as the solvent and matrix, respectively.

GdmCl buffer, typically 8 M, has been frequently used to dissolve Sup35NM to make a relatively concentrated solution and then the solution diluted to initiate protein association,[36,50,51] in which the lack of formation of β-sheet checked by the fluorescence method was often used to illustrate protein dissolution. However, such a method cannot detect a trace amount of oligomers without β-sheet in the solution mixture. Recently, our LLS study revealed that even at such a high GdmCl buffer concentration (8 M), a small amount of oligomers exist which could act as seeds to nucleate oligomerization and fibril formation. In addition, we found that these small oligomers can be effectively removed by slowly passing the protein solution through a 20 nm membrane at a flow rate of 1 mL/h.[52]

In this study, we used such a pretreatment procedure, and the results are summarized in Figure 3. Before the filtration with a 20 nm membrane, there are two peaks. One corresponds to the hydrodynamic radius distribution of individual protein or conjugated chains, while another located at ~10^2 nm reflects protein aggregation. It should be noted that the number of aggregates is very small because the distribution is weighted by

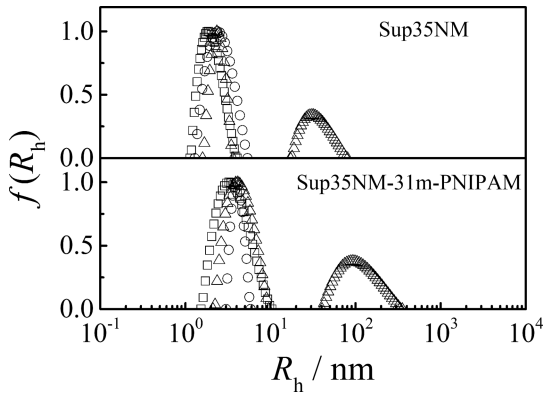

Figure 3. Dynamic LLS results of wild-type Sup35NM and the Sup35NM-31m−PNIPAM conjugate in 8 M GdmCl buffer before (△, 1.5 mg/mL) and after (○, 1.4 mg/mL) the solution had been passed through a 20 nm membrane filter, and after further concentration by ultrafiltration (□, 17 mg/mL), where protein concentrations were measured by the BCA protein assay.

the scattered light intensity that is proportional to the square of the mass of scattering objects. Ultrafiltration removes the second peak even in the concentrated solution and enables us to have a well-defined starting point in the study of the initial oligomerization.

ThT Fluorescence Assay and TEM Studies. The aggregation of Sup35NM *in vitro* is generally recognized as a two-stage process.[62,63] In the first lag phase, Sup35NM monomers are slowly associated into small oligomers (intermediates) or "nuclei" (lag phase), and in the second cascade process, each nucleus induces the formation of amyloid fibers (fibril propagation). To classify these two stages, a ThT fluorescence assay has long been developed as a regular method for detecting the β-sheets formed inside amyloid fibrils. Figure 4 shows that the ThT fluorescence intensity starts to increase

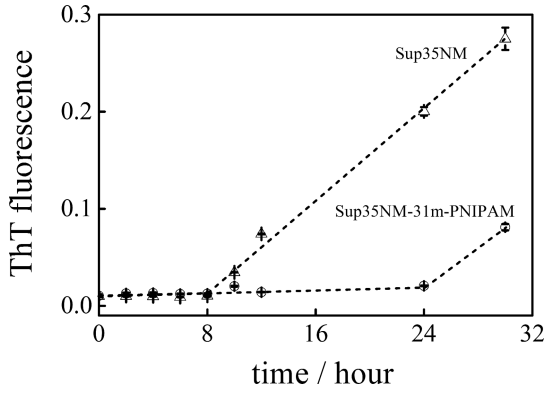

Figure 4. Time dependence of the fluorescence intensity of Sup35NM and the Sup35NM-31m−PNIPAM conjugate after 200-fold dilution from 8 M GdmCl into PBS, where the final protein and ThT dye concentrations are 3 and 10 μM, respectively. Each point was measured in triplicate and is presented as the mean ± the standard deviation. The fluorescence intensity is normalized by its corresponding maximum value. The dashed lines are drawn to guide the eye.

~12 h after the dilution from denaturant GdmCl into PBS for wild-type Sup35NM, but a similar fluorescence intensity increase does not occur until ~24 h for the Sup35NM-31m−PNIPAM conjugate. Therefore, conjugation prolongs the time window, which enables us to study the lag phase under the current experimental conditions.

To quantify the inhibition effect of the conjugation on the oligomerization of Sup35NM, we used the Fink−Watzky (F−W) two-step model to analyze the aggregation kinetic data in Figure 4. The aggregation is simplified into two steps: a slow nucleation step (A → B) with a rate constant k_1 and a fast autocatalytic step (A + B → 2B) with a rate constant k_2, described as[64,65]

$$[\mathrm{B}]_t = [\mathrm{A}]_0 - \frac{\frac{k_1}{k_2} + [\mathrm{A}]_0}{1 + \frac{k_1}{k_2[\mathrm{A}]_0}\exp(k_1 + k_2[\mathrm{A}]_0)t} \quad (5)$$

where $[\mathrm{B}]_t$ and $[\mathrm{A}]_0$ represent the concentration of aggregation product at time t and the initial protein monomer concentration, respectively.

Figure 5 shows that eq 5 fits the data well with a k_1 of 5.0 × 10^{-3} h^{-1} and a k_2 of 3.0 × 10^{-2} μM^{-1} h^{-1} for wild-type Sup35NM, while for the Sup35NM-31m−PNIPAM conjugate, k_1 = 1.5 × 10^{-3} h^{-1} and k_2 = 1.8 × 10^{-2} μM^{-1} h^{-1}. Clearly, the Sup35NM-31m−PNIPAM conjugate has k_1 and k_2 values that

DOI: 10.1021/acs.biochem.7b00966
Biochemistry 2017, 56, 6575−6584

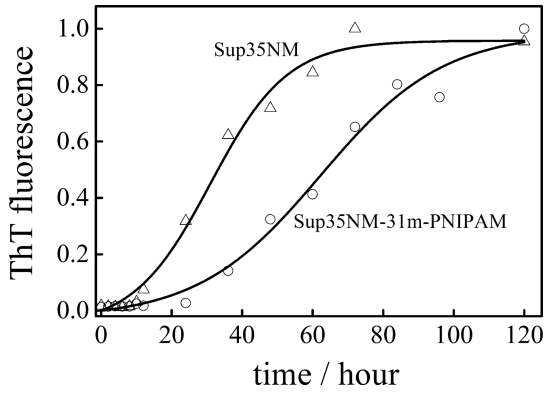

Figure 5. Time dependence of fluorescence intensity of wild-type Sup35NM and the Sup35NM-31m−PNIPAM conjugate after 200-fold dilution of their respective solutions in 8 M GdmCl into PBS, where the final protein concentration is 3 μM. Fluorescence intensities are normalized by their corresponding maximum value. The solid lines represent the F−W model fitting with $R^2 \geq 0.98$.

are smaller than those of wild-type Sup35NM, indicating that the conjugation of PNIPAM to Sup35NM not only retards the lag phase >2-fold but also slows fibril formation. On the basis of the fact that there are intermolecular interactions between the 31st residues on protein Sup35NM during the protein association process,[23] conjugation of the PNIAM chain at its 31st residue will introduce steric hindrance and interfere the intermolecular association, which finally results in slower aggregation kinetics. In addition, we used TEM to analyze the morphology of the fibrils and fibers evidenced by the ThT fluorescence assay.

Figure 6 shows the typical TEM results of both wild-type Sup35NM and the Sup35NM-31m−PNIPAM conjugate 80 h

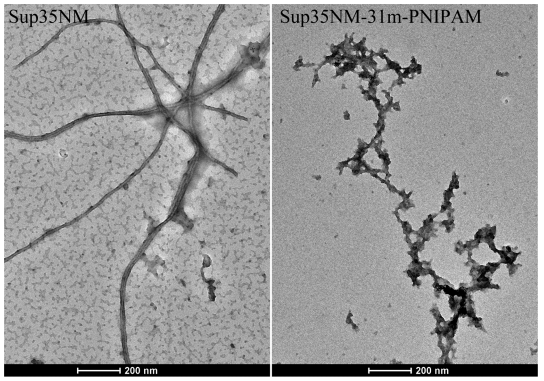

Figure 6. Typical TEM images of aggregates of wild-type Sup35NM and the Sup35NM-31m−PNIPAM conjugate after 200-fold dilution of their respective solutions in 8 M GdmCl into PBS at 25 °C, where the final protein concentration is 3 μM. The TEM picture was taken 80 h after dilution.

after the dilution, where long amyloid-like fibrils are formed in the solution of wild-type Sup35NM, while only short irregular aggregates are seen for the Sup35NM-31m−PNIPAM conjugate. Namely, conjugation affects fibril formation, confirming the results obtained from the ThT fluorescence assay. It is worth noting that we used liquid nitrogen to quickly freeze a drop of the solution and then removed the solvent by freeze-drying,[55] which fixes the morphology in the solution state so that further oligomerization or aggregation is avoided during the solvent evaporation process. Such a combination of this special sample preparation and TEM enables us to imitate cryo-TEM.

LLS Analysis of the Oligomerization of Sup35NM and the Sup35NM-31m−PNIPAM Conjugate. As stated previously, the ThT fluorescence assay detects the formation of only β-sheets but not nonstructured oligomers. The fluorescence intensity in Figure 4 shows no change during the lag phases (first ~12 h for Sup35NM and ~24 h for the Sup35NM-31m−PNIPAM conjugate). To observe the formation of the protein oligomers without or with a small amount of β-sheets formed during the lag phase, we used a combination of static and dynamic LLS to study the initial limited chain association (oligomerization) because it is extremely sensitive to the molar mass change of the scattering objects, irrespective of the formation of β-sheets. Here, we concentrated on the initial time window of 12 h because wild-type Sup35NM starts to form large aggregates with detectable β-sheets, as shown in Figure 4. For comparison with the results obtained in the ThT fluorescence assay study, we maintained an identical experimental condition in LLS experiments.

Figure 7 shows that the average scattered light intensity of wild-type Sup35NM also increases faster than that of the

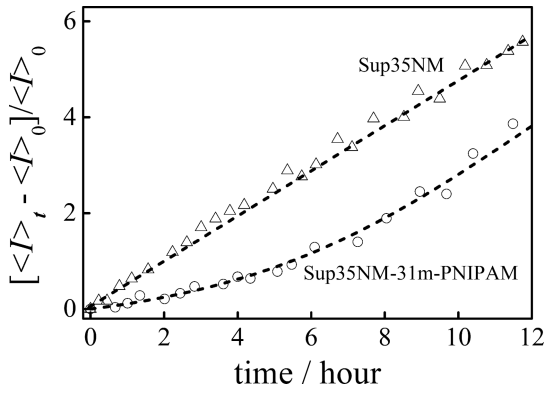

Figure 7. Time dependence of excess average scattered light intensity of Sup35NM and the Sup35NM-31m−PNIPAM conjugate after 200-fold dilution of their respective solutions in 8 M GdmCl into PBS at 25 °C, where the final protein concentration is 3 μM and the scattering angle is 30°. The dashed lines are guides for the eye.

Sup35NM-31m−PNIPAM conjugate during the first 12 h after the dilution to initiate protein association. It should be noted that the average scattered light intensity of the Sup35NM-31m−PNIPAM conjugate nearly remains a constant in the first 2 h, indicating that the oligomerization is practically stopped or significantly slowed during the initial lag phase, enabling us to use this stable time window to study effects of adding small molecular drugs on the lag phase kinetics.

For comparison, we also studied how free PNIPAM chains affect the association of wild-type Sup35NM by LLS. Figure 8 shows that free PNIPAM chains actually promote the association of wild-type Sup35NM, which is the opposite of what is seen for the Sup35NM-31m−PNIPAM conjugate to which PNIPAM is covalently linked.

On the basis of the result presented above, we are able to use this conjugating method to screen out those small molecular drugs that can slow the initial oligomerization or, in other words, prolong the lag phase. Clinically, we can use some of these drugs to delay, not stop or reverse as people have tried to

DOI: 10.1021/acs.biochem.7b00966
Biochemistry 2017, 56, 6575−6584

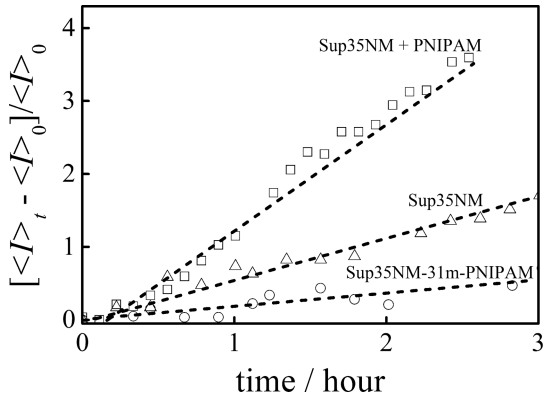

Figure 8. Time dependence of excess average scattered light intensity of the Sup35NM-31m−PNIPAM conjugate (○), wild-type Sup35NM (△), and a 1:1 Sup35NM/PNIPAM mixture (□) after 200-fold dilution from 8 M GdmCl into PBS at 25 °C, where the final protein concentration is 3 μM. The 1:1 Sup35NM/PNIPAM mixture was prepared by mixing and then filtration with a 0.22 μm membrane. The dashed lines are guides for the eye.

do, the occurrence of a neuron degenerative disease. To use the oligomerization kinetics to screen out potential drugs that can slow the initial lag phase, we have to make sure that the measured kinetics is repeatable. To do so, we repeated the dilution of a denatured Sup35NM-31m−PNIPAM conjugate concentrated solution into PBS to initiate protein association.

Figure 9 shows that in the first 6 h, three repeated experimental results fall on top of each other, indicating that

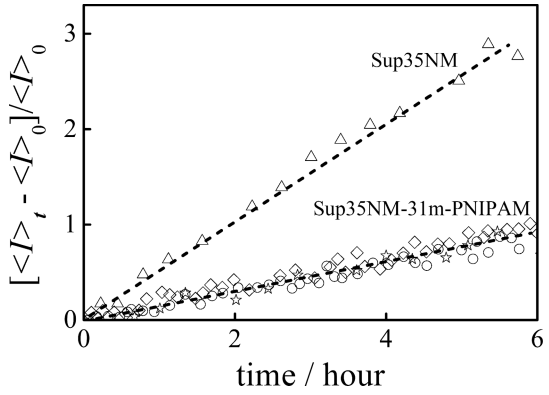

Figure 9. Time dependence of the excess average scattered light intensity of Sup35NM and the Sup35NM-31m−PNIPAM conjugate (three repeated measurements, ○, □, and ☆) after 200-fold dilution from 8 M GdmCl into PBS at 25 °C, where the final protein concentration is 3 μM. The dashed lines are guides for the eye.

we can use this repeatable initial kinetics to screen potential small molecular drugs to see which ones can further slow the oligomerization kinetics. In comparison with wild-type Sup35NM, the Sup35NM-31m−PNIPAM conjugate chains associate with each other at a much slower rate in the first 6 h, and the average scattered light intensity increases only ~1-fold after 6 h.

Data Fitting of LLS Results with the Oligomerization Process. On the basis of our LLS results (scattered light intensity increase), we are able to estimate the oligomer distribution of the Sup35NM-31m−PNIPAM conjugate by using the Smoluchowski coagulation equation. Assuming that (1) the association rate constant $K_{i,j}$ for two oligomers made of i and j monomers is similar for any pair of oligomers (i.e., $K_{i,j} = K_{j,i}$), (2) the association of two oligomers is irreversible, and (3) the simultaneous association of three or more oligomers is omitted because of its low probability in dilute solution, we have[66]

$$\frac{\mathrm{d}}{\mathrm{d}t}N_k(t) = \frac{1}{2}\sum_{i+j=k} K_{i,j}N_i(t)N_j(t) - N_k(t)\sum_{j=1}^{\infty} K_{k,j}N_j(t) \tag{6}$$

where $N_k(t)$ is the number concentration of oligomers made of k monomers (denoted as k-mer hereafter) at time t. Equation 6 can be rewritten as

$$\frac{\mathrm{d}}{N_1(0)\,\mathrm{d}t}n_k(t) = \frac{1}{2}\sum_{i+j=k} K_{i,j}n_i(t)n_j(t) - n_k(t)\sum_{j=1}^{\infty} K_{k,j}n_j(t) \tag{7}$$

where $N_1(0)$ is the initial number concentration of protein chains and $n_k(t)$ is the $N_1(0)$-normalized number concentration of clusters with k protein chains, i.e., $\Sigma_i i n_i = 1$. For a diffusion-limited association, $K_{i,j}$ for diffusive oligomers is given by[67]

$$K_{i,j} = 4\pi(R_i + R_j)(D_i + D_j) \tag{8}$$

where R_i and D_i are the hydrodynamic radius and translational diffusion coefficient of an i-mer, respectively. On the basis of polymer physics, R_i is scaled to i (i.e., mass) as $R_i \sim i^{\beta}$ and R is related to D by the Stokes−Einstein equation, so that $K_{i,j}$ is a function of i and j with a scaling constant β and other constants (solvent viscosity η and temperature T). The numerical solution of such a Smoluchowski coagulation equation showed that $n_i(t)$ and its average value, $\langle n_i(t)\rangle$, deviate no more than 5% from those obtained using $K_{i,j} = \alpha k_s$ in the initial association stage,[67] where $0 < \alpha \leq 1$ is the sticking probability and k_s is a constant related to η and T. Therefore, $K_{i,j}$ in eq 7 can be taken out of those summations, moved to the left, and combined with $N_1(0)$ and t as a rescaled time τ. For example

$$\frac{\mathrm{d}}{\mathrm{d}\tau}n_k(\tau) = \frac{1}{2}\sum_{i+j=k} n_i(\tau)n_j(\tau) - n_k(\tau)\sum_{j=1}^{\infty} n_j(\tau) \tag{9}$$

where $\tau = [\alpha k_s N_1(0)]t = \gamma_s t$, with $\gamma_s = \alpha k_s N_1(0)$, a constant. Equation 9 can be solved analytically with a solution as follows[68,69]

$$n_i(\tau) = (\tau/2)^{i-1}/(1 + \tau/2)^{i+1} \tag{10}$$

On the basis of static LLS theory, at sufficiently lower c and q values, we have

$$\frac{\langle I_t\rangle}{\langle I_0\rangle} = \frac{M_w(t)}{M_1} = \frac{\sum_i w_i M_i}{M_1} = \frac{\sum_i [n_i i M_1/(1 \times M_1)] \times i M_1}{M_1} = \sum_i i^2 n_i = 1 + \tau \tag{11}$$

where w_i is the normalized weight distribution of the i-mer and M_1 is the molar mass of individual protein chains. Therefore, the intensity ratio of the left side of eq 11 is proportional to t, as shown in Figure 10, where the slope leads to a γ_s of 0.156 h^{-1}. Note that $k_s = 8k_BT/3\eta = 7.4 \times 10^9$ M^{-1} s^{-1} at 298.15 K in PBS, so that $\alpha = 2 \times 10^{-9}$, indicating that most collisions

DOI: 10.1021/acs.biochem.7b00966
Biochemistry 2017, 56, 6575−6584

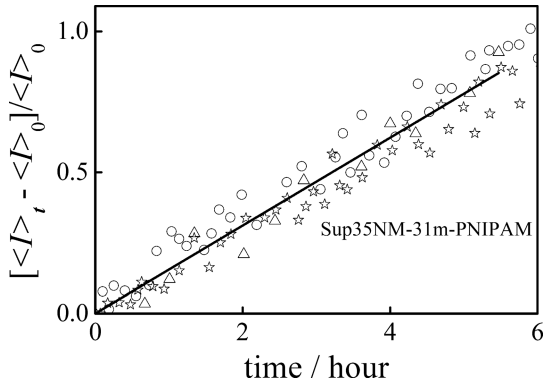

Figure 10. Time dependence of the normalized excess average scattered light intensity of the Sup35NM-31m−PNIPAM conjugate (data from Figure 9), where the line represents a fit of eq 11 with $R^2 \geq 0.98$.

between two protein chains or oligomers lead to no interchain association when $N_1(0)$ is only 3 μM.

Figure 11 shows the time dependence of the oligomer distribution $[n_i(t)]$ on the basis of eq 10, where the inset reveals

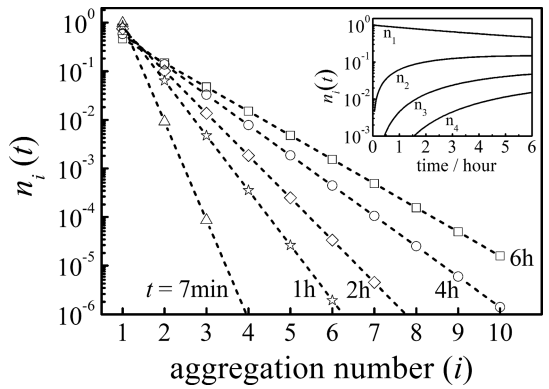

Figure 11. Calculated oligomer distribution of the conjugates at different time intervals based on the Smoluchowski coagulation equation. The dashed lines are guides for the eye. The inset shows the calculated time-dependent percentage of $n_i(t)$.

the time-dependent percentage of $n_i(t)$. It shows that even after 6 h, ~47% of protein chains $[N_1(0)]$ remain as individual chains (monomer) and ~30, ~15, and ~6% of protein chains exist as dimers, trimers, and tetramers, respectively. The oligomers with a higher association number make up <2%. A combination of LLS results and Smoluchowski coagulation analysis clearly reveals that in the initial stage of oligomerization, most proteins remain as individual chains, and this provides us with a repeatable and quantitative protocol for studying the oligomerization kinetics. More importantly, using such an established protocol, we are able to study the effects of different small molecules on the oligomerization kinetics and screen out some potential drugs. The currently used neuron drugs are the first batch on our testing list.

CONCLUSIONS

The site-specific conjugation of a short thermally sensitive PNIPAM chain to a model protein Sup35NM is an effective way to slow protein association kinetics (both in the initial oligomerization, i.e., the lag phase, and in the subsequent fibril formation). Using this conjugation method, we are able to arrest the initial oligomerization kinetics of Sup35NM after its dilution in PBS for at least 2 h. Moreover, the oligomerization kinetics could be further regulated via the solution temperature because of PNIPAM's unique thermal sensitivity. Combining LLS results and Smoluchowski coagulation analysis, we have successfully developed a repeatable and quantitative protocol for studying the oligomerization kinetics. Such a quantitative and repeatable protocol enables us to reliably evaluate and screen out potential drugs that can effectively prolong the lag phase of neurodegenerative diseases. However, caution is needed when applying this method because false positives that interact with only conjugated PNIPAM will also prevent the formation of nuclei. A second screen might be needed to exclude this situation. Nevertheless, it is a promising method that enables us to study the initial protein association in detail and can be easily transferred to other pathogenic proteins where there is a −SH group (native or engineered) by using thiol−ene click chemistry. In summary, instead of stopping or reversing protein fibril formation, we are trying to establish a new strategy in which we can use small molecular drugs to prolong the lag phase (oligomerization) so that the neurodegenerative diseases are not be able to severely develop during the lifetimes of patients. Ideally, if such drugs could be found, potential patients should take them years before the development of any disease to slow the development of potential neurodegenerative diseases so that their quality of life could be significantly improved. We are hopeful that our current study can stimulate more research activity in this area.

AUTHOR INFORMATION

Corresponding Author

*E-mail: wangyanjing@link.cuhk.edu.hk.

ORCID

Yanjing Wang: 0000-0001-6395-1872

Funding

This work was supported by the Hong Kong Special Administration Region Earmarked Projects (CUHK4042/13P, 2130349, and 4053060).

Notes

The authors declare no competing financial interest.

ACKNOWLEDGMENTS

Y.W. specially thanks Dr. Shu Diao and Dr. Hong Zhao for their kind help when she started this project.

REFERENCES

(1) Dobson, C. M. (2003) Protein folding and misfolding. *Nature 426*, 884−890.

(2) Dill, K. A., and MacCallum, J. L. (2012) The Protein-Folding Problem, 50 Years On. *Science 338*, 1042−1046.

(3) Soto, C. (2003) Unfolding the role of protein misfolding in neurodegenerative diseases. *Nat. Rev. Neurosci. 4*, 49−60.

(4) Schroder, C., Steinhauser, O., Sasisanker, P., and Weingartner, H. (2015) Orientational alignment of amyloidogenic proteins in pre-aggregated solutions. *Phys. Rev. Lett. 114*, 128101.

(5) Yoshimura, Y., So, M., Yagi, H., and Goto, Y. (2013) Ultrasonication: An Efficient Agitation for Accelerating the Supersaturation-Limited Amyloid Fibrillation of Proteins. *Jpn. J. Appl. Phys. 52*, 07HA01.

(6) Lotz, G. P., and Legleiter, J. (2013) The role of amyloidogenic protein oligomerization in neurodegenerative disease. *J. Mol. Med. 91*, 653−664.

DOI: 10.1021/acs.biochem.7b00966
Biochemistry 2017, 56, 6575−6584

(7) Lindner, A. B., and Demarez, A. (2009) Protein aggregation as a paradigm of aging. *Biochim. Biophys. Acta, Gen. Subj. 1790*, 980−996.
(8) Teoh, C. L., Su, D., Sahu, S., Yun, S.-W., Drummond, E., Prelli, F., Lim, S., Cho, S., Ham, S., Wisniewski, T., and Chang, Y.-T. (2015) Chemical Fluorescent Probe for Detection of Aβ Oligomers. *J. Am. Chem. Soc. 137*, 13503−13509.
(9) Berry, D. B., Lu, D., Geva, M., Watts, J. C., Bhardwaj, S., Oehler, A., Renslo, A. R., DeArmond, S. J., Prusiner, S. B., and Giles, K. (2013) Drug resistance confounding prion therapeutics. *Proc. Natl. Acad. Sci. U. S. A. 110*, E4160−E4169.
(10) Zhang, X., Tian, Y., Li, Z., Tian, X., Sun, H., Liu, H., Moore, A., and Ran, C. (2013) Design and synthesis of curcumin analogues for in vivo fluorescence imaging and inhibiting copper-induced cross-linking of amyloid beta species in Alzheimer's disease. *J. Am. Chem. Soc. 135*, 16397−16409.
(11) Feng, B. Y., Toyama, B. H., Wille, H., Colby, D. W., Collins, S. R., May, B. C., Prusiner, S. B., Weissman, J., and Shoichet, B. K. (2008) Small-molecule aggregates inhibit amyloid polymerization. *Nat. Chem. Biol. 4*, 197−199.
(12) Young, L. M., Saunders, J. C., Mahood, R. A., Revill, C. H., Foster, R. J., Tu, L. H., Raleigh, D. P., Radford, S. E., and Ashcroft, A. E. (2015) Screening and classifying small-molecule inhibitors of amyloid formation using ion mobility spectrometry-mass spectrometry. *Nat. Chem. 7*, 73−81.
(13) Wagner, J., Ryazanov, S., Leonov, A., Levin, J., Shi, S., Schmidt, F., Prix, C., Pan-Montojo, F., Bertsch, U., Mitteregger-Kretzschmar, G., Geissen, M., Eiden, M., Leidel, F., Hirschberger, T., Deeg, A. A., Krauth, J. J., Zinth, W., Tavan, P., Pilger, J., Zweckstetter, M., Frank, T., Bähr, M., Weishaupt, J. H., Uhr, M., Urlaub, H., Teichmann, U., Samwer, M., Bötzel, K., Groschup, M., Kretzschmar, H., Griesinger, C., and Giese, A. (2013) Anle138b: a novel oligomer modulator for disease-modifying therapy of neurodegenerative diseases such as prion and Parkinson's disease. *Acta Neuropathol. 125*, 795−813.
(14) Zhang, H., Xu, L.-Q., and Perrett, S. (2011) Studying the effects of chaperones on amyloid fibril formation. *Methods 53*, 285−294.
(15) Yang, F., Lim, G. P., Begum, A. N., Ubeda, O. J., Simmons, M. R., Ambegaokar, S. S., Chen, P. P., Kayed, R., Glabe, C. G., Frautschy, S. A., and Cole, G. M. (2005) Curcumin inhibits formation of amyloid β oligomers and fibrils, binds plaques, and reduces amyloid in vivo. *J. Biol. Chem. 280*, 5892−5901.
(16) Ritchie, C. W., Bush, A. I., Mackinnon, A., Macfarlane, S., Mastwyk, M., MacGregor, L., Kiers, L., Cherny, R., Li, Q. X., Tammer, A., Carrington, D., Mavros, C., Volitakis, I., Xilinas, M., Ames, D., Davis, S., Beyreuther, K., Tanzi, R. E., and Masters, C. L. (2003) Metal-protein attenuation with iodochlorhydroxyquin (clioquinol) targeting aβ amyloid deposition and toxicity in alzheimer disease: A pilot phase 2 clinical trial. *Arch. Neurol. 60*, 1685−1691.
(17) Lorenzo, A., and Yankner, B. A. (1994) Beta-amyloid neurotoxicity requires fibril formation and is inhibited by congo red. *Proc. Natl. Acad. Sci. U. S. A. 91*, 12243−12247.
(18) Blanchard, B. J., Chen, A., Rozeboom, L. M., Stafford, K. A., Weigele, P., and Ingram, V. M. (2004) Efficient reversal of Alzheimer's disease fibril formation and elimination of neurotoxicity by a small molecule. *Proc. Natl. Acad. Sci. U. S. A. 101*, 14326−14332.
(19) Mangione, M. R., Vilasi, S., Marino, C., Librizzi, F., Canale, C., Spigolon, D., Bucchieri, F., Fucarino, A., Passantino, R., Cappello, F., Bulone, D., and San Biagio, P. L. (2016) Hsp60, amateur chaperone in amyloid-beta fibrillogenesis. *Biochim. Biophys. Acta, Gen. Subj. 1860*, 2474−2483.
(20) Liu, Y., Wei, H., Wang, J., Qu, J., Zhao, W., and Tao, H. (2007) Effects of randomizing the Sup35NM prion domain sequence on formation of amyloid fibrils in vitro. *Biochem. Biophys. Res. Commun. 353*, 139−146.
(21) Carballo-Pacheco, M., and Strodel, B. (2016) Advances in the Simulation of Protein Aggregation at the Atomistic Scale. *J. Phys. Chem. B 120*, 2991−2999.
(22) Carrotta, R., Canale, C., Diaspro, A., Trapani, A., Biagio, P. L. S., and Bulone, D. (2012) Inhibiting effect of αs1-casein on Aβ1−40 fibrillogenesis. *Biochim. Biophys. Acta, Gen. Subj. 1820*, 124−132.
(23) Krishnan, R., and Lindquist, S. L. (2005) Structural insights into a yeast prion illuminate nucleation and strain diversity. *Nature 435*, 765−772.
(24) Knowles, T. P. J., Vendruscolo, M., and Dobson, C. M. (2015) The physical basis of protein misfolding disorders. *Phys. Today 68*, 36−41.
(25) Baldwin, A. J., Knowles, T. P. J., Tartaglia, G. G., Fitzpatrick, A. W., Devlin, G. L., Shammas, S. L., Waudby, C. A., Mossuto, M. F., Meehan, S., Gras, S. L., Christodoulou, J., Anthony-Cahill, S. J., Barker, P. D., Vendruscolo, M., and Dobson, C. M. (2011) Metastability of Native Proteins and the Phenomenon of Amyloid Formation. *J. Am. Chem. Soc. 133*, 14160−14163.
(26) Knowles, T. P. J., Vendruscolo, M., and Dobson, C. M. (2014) The amyloid state and its association with protein misfolding diseases. *Nat. Rev. Mol. Cell Biol. 15*, 384−396.
(27) Jarrett, J. T., and Lansbury, P. T. (1993) Seeding "one-dimensional crystallization" of amyloid: A pathogenic mechanism in Alzheimer's disease and scrapie? *Cell 73*, 1055−1058.
(28) Currais, A., Fischer, W., Maher, P., and Schubert, D. (2017) Intraneuronal protein aggregation as a trigger for inflammation and neurodegeneration in the aging brain. *FASEB J. 31*, 5−10.
(29) Heiser, V., Engemann, S., Bröcker, W., Dunkel, I., Boeddrich, A., Waelter, S., Nordhoff, E., Lurz, R., Schugardt, N., Rautenberg, S., Herhaus, C., Barnickel, G., Böttcher, H., Lehrach, H., and Wanker, E. E. (2002) Identification of benzothiazoles as potential polyglutamine aggregation inhibitors of Huntington's disease by using an automated filter retardation assay. *Proc. Natl. Acad. Sci. U. S. A. 99*, 16400−16406.
(30) Biancalana, M., and Koide, S. (2010) Molecular mechanism of Thioflavin-T binding to amyloid fibrils. *Biochim. Biophys. Acta, Proteins Proteomics 1804*, 1405−1412.
(31) Hudson, S. A., Ecroyd, H., Kee, T. W., and Carver, J. A. (2009) The thioflavin T fluorescence assay for amyloid fibril detection can be biased by the presence of exogenous compounds. *FEBS J. 276*, 5960−5972.
(32) Rambaran, R. N., and Serpell, L. C. (2008) Amyloid fibrils: Abnormal protein assembly. *Prion 2*, 112−117.
(33) Narayanan, S., Walter, S., and Reif, B. (2006) Yeast prion-protein, sup35, fibril formation proceeds by addition and substraction of oligomers. *ChemBioChem 7*, 757−765.
(34) Chen, C. Y., Rojanatavorn, K., Clark, A. C., and Shih, J. C. (2005) Characterization and enzymatic degradation of Sup35NM, a yeast prion-like protein. *Protein Sci. 14*, 2228−2235.
(35) Bagriantsev, S. N., Gracheva, E. O., Richmond, J. E., and Liebman, S. W. (2008) Variant-specific [PSI(+)] Infection Is Transmitted by Sup35 Polymers within [PSI(+)] Aggregates with Heterogeneous Protein Composition. *Mol. Biol. Cell 19*, 2433−2443.
(36) Glover, J. R., Kowal, A. S., Schirmer, E. C., Patino, M. M., Liu, J.-J., and Lindquist, S. (1997) Self-Seeded Fibers Formed by Sup35, the Protein Determinant of [PSI+], a Heritable Prion-like Factor of S. cerevisiae. *Cell 89*, 811−819.
(37) Balbirnie, M., Grothe, R., and Eisenberg, D. S. (2001) An amyloid-forming peptide from the yeast prion Sup35 reveals a dehydrated beta-sheet structure for amyloid. *Proc. Natl. Acad. Sci. U. S. A. 98*, 2375−2380.
(38) Serio, T. R., Cashikar, A. G., Moslehi, J. J., Kowal, A. S., and Lindquist, S. L. (1999) Yeast prion [Ψ+] and its determinant, sup35p. In *Methods in Enzymology*, pp 649−673, Academic Press, San Diego.
(39) Maeda, Y., and Matsui, H. (2012) Genetically engineered protein nanowires: unique features in site-specific functionalization and multi-dimensional self-assembly. *Soft Matter 8*, 7533.
(40) Hoffman, A. S. (2000) Bioconjugates of Intelligent Polymers and Recognition Proteins for Use in Diagnostics and Affinity Separations. *Clin. Chem. 46*, 1478−1486.
(41) Li, M., De, P., Li, H., and Sumerlin, B. S. (2010) Conjugation of RAFT-generated polymers to proteins by two consecutive thiol−ene reactions. *Polym. Chem. 1*, 854.
(42) Wu, C., and Zhou, S. (1995) Laser light scattering study of the phase transition of poly (N-isopropylacrylamide) in water. 1. Single chain. *Macromolecules 28*, 8381−8387.

DOI: 10.1021/acs.biochem.7b00966
Biochemistry 2017, 56, 6575−6584

(43) Wu, C., and Zhou, S. (1995) Thermodynamically stable globule state of a single poly (N-isopropylacrylamide) chain in water. *Macromolecules 28*, 5388−5390.
(44) Chan, J. W., Hoyle, C. E., Lowe, A. B., and Bowman, M. (2010) Nucleophile-Initiated Thiol-Michael Reactions: Effect of Organocatalyst, Thiol, and Ene. *Macromolecules 43*, 6381−6388.
(45) Li, G.-Z., Randev, R. K., Soeriyadi, A. H., Rees, G., Boyer, C., Tong, Z., Davis, T. P., Becer, C. R., and Haddleton, D. M. (2010) Investigation into thiol-(meth)acrylate Michael addition reactions using amine and phosphine catalysts. *Polym. Chem. 1*, 1196.
(46) Brosnan, S. M., and Schlaad, H. (2014) Modification of polypeptide materials by Thiol-X chemistry. *Polymer 55*, 5511−5516.
(47) Heredia, K. L., and Maynard, H. D. (2007) Synthesis of protein-polymer conjugates. *Org. Biomol. Chem. 5*, 45−53.
(48) Jung, B., and Theato, P. (2013) Chemical Strategies for the Synthesis of Protein−Polymer Conjugates. In *Bio-synthetic Polymer Conjugates* (Schlaad, H., Ed.) pp 37−70, Springer, Berlin.
(49) Soto, C., and Estrada, L. D. (2008) Protein misfolding and neurodegeneration, fibrils formation is a pretective mechanism. *Arch. Neurol. 65*, 184−189.
(50) Hess, S., Lindquist, S. L., and Scheibel, T. (2007) Alternative assembly pathways of the amyloidogenic yeast prion determinant Sup35-NM. *EMBO Rep. 8*, 1196−1201.
(51) Palhano, F. L., Rocha, C. B., Bernardino, A., Weissmuller, G., Masuda, C. A., Montero-Lomeli, M., Gomes, A. M., Chien, P., Fernandes, P. M., and Foguel, D. (2009) A fluorescent mutant of the NM domain of the yeast prion Sup35 provides insight into fibril formation and stability. *Biochemistry 48*, 6811−6823.
(52) Diao, S., Zhao, H., Wang, W., and Wu, C. (2012) Preparation of true solutions of monomeric amyloidogenic protein/peptide: A critical prerequisite for aggregation kinetic study. *Sci. China: Chem. 55*, 118−124.
(53) Lundmark, K., Westermark, G. T., Olsen, A., and Westermark, P. (2005) Protein fibrils in nature can enhance amyloid protein A amyloidosis in mice: Cross-seeding as a disease mechanism. *Proc. Natl. Acad. Sci. U. S. A. 102*, 6098−6102.
(54) LeVine, H. (1993) Thioflavine T interaction with synthetic Alzheimer's disease beta-amyloid peptides: detection of amyloid aggregation in solution. *Protein Sci. 2*, 404−410.
(55) Zhao, H., Chen, Q., Hong, L., Zhao, L., Wang, J., and Wu, C. (2011) What Morphologies Do We Want? - TEM Images from Dilute Diblock Copolymer Solutions. *Macromol. Chem. Phys. 212*, 663−672.
(56) Chu, B. (1991) *Laser Light Scattering: Basic Principles and Practice*, Academic Press, San Diego.
(57) Iwao, T. (2002) *Polymer solutions: An introduction to physical properties*, Wiley, New York.
(58) Berne, B. J., and Pecora, R. (2000) *Dynamic light scattering: With applications to chemistry, biology, and physics*, Courier Dover Publications, Mineola, NY.
(59) Heredia, K. L., Bontempo, D., Ly, T., Byers, J. T., Halstenberg, S., and Maynard, H. D. (2005) In Situ Preparation of Protein−"Smart" Polymer Conjugates with Retention of Bioactivity. *J. Am. Chem. Soc. 127*, 16955−16960.
(60) Jones, M. W., Mantovani, G., Ryan, S. M., Wang, X., Brayden, D. J., and Haddleton, D. M. (2009) Phosphine-mediated one-pot thiol−ene "click" approach to polymer−protein conjugates. *Chem. Commun. (Cambridge, U. K.)*, 5272−5274.
(61) Stenzel, M. H. (2013) Bioconjugation Using Thiols: Old Chemistry Rediscovered to Connect Polymers with Nature's Building Blocks. *ACS Macro Lett. 2*, 14−18.
(62) Scheibel, T., Bloom, J., and Lindquist, S. L. (2004) The elongation of yeast prion fibers involves separable steps of association and conversion. *Proc. Natl. Acad. Sci. U. S. A. 101*, 2287−2292.
(63) Serio, T. R., Cashikar, A. G., Kowal, A. S., Sawicki, G. J., Moslehi, J. J., Serpell, L., Arnsdorf, M. F., and Lindquist, S. L. (2000) Nucleated Conformational Conversion and the Replication of Conformational Information by a Prion Determinant. *Science 289*, 1317−1321.
(64) Morris, A. M., Watzky, M. A., Agar, J. N., and Finke, R. G. (2008) Fitting Neurological Protein Aggregation Kinetic Data via a 2-Step, Minimal/"Ockham's Razor" Model: The Finke−Watzky Mechanism of Nucleation Followed by Autocatalytic Surface Growth. *Biochemistry 47*, 2413−2427.
(65) Watzky, M. A., Morris, A. M., Ross, E. D., and Finke, R. G. (2008) Fitting Yeast and Mammalian Prion Aggregation Kinetic Data with the Finke−Watzky Two-Step Model of Nucleation and Autocatalytic Growth. *Biochemistry 47*, 10790−10800.
(66) Smoluchowski, M. v. (1918) Versuch einer mathematischen Theorie der Koagulationskinetik kolloider Lösungen. *Z. Phys. Chem. 92*, 129−168.
(67) Modler, A. J., Gast, K., Lutsch, G., and Damaschun, G. (2003) Assembly of Amyloid Protofibrils via Critical Oligomers—A Novel Pathway of Amyloid Formation. *J. Mol. Biol. 325*, 135−148.
(68) Feder, J., Jøssang, T., and Rosenqvist, E. (1984) Scaling Behavior and Cluster Fractal Dimension Determined by Light Scattering from Aggregating Proteins. *Phys. Rev. Lett. 53*, 1403−1406.
(69) Dubovskiĭ, P. B. (1994) *Mathematical Theory of Coagulation*, Research Institute of Mathematics, Global Analysis Research Center, Seoul National University, Seoul.

DOI: 10.1021/acs.biochem.7b00966
Biochemistry 2017, 56, 6575−6584